Intermetallic Strengthened Alumina-Forming Austenitic Steels for Energy Applications

Bin Hu, Geneva Trotter, Ian Baker

Thayer School of Engineering, Dartmouth College, Hanover, NH 03755

DOE grant DE-FE0008857

Acknowledgement

- Professors at Dartmouth College:
  - Erland M. Schulson, Ph.D.
  - Harold J. Frost, Ph.D.
- Dr. Charles Daghlian in EM Facility at Dartmouth College
- Dr. Yukinori Yamamoto, Dr. Michael Brady and Dr. Michael Miller at Oak Ridge National Laboratory
- Dr. Si Chen and Dr. Zhonghou Cai in Argonne National Laboratory
- Professors, colleagues and friends at Dartmouth College
- Funded by the U.S. Department of Energy NETL Award DEFG2612FE0008857

Outline

- Introduction
  - Motivation
  - Background
- Results and Discussion
  - Microstructural analysis
  - Thermomechanical treatments
  - SEM & TEM characterization
  - XRD analysis
  - Room temperature tensile tests
- Summary

New Materials for High Temperature Applications

- **Motivation**: Develop materials which can be used at higher temperature (>700 °C) and pressure (>100 MPa) to enhance efficiency (>50 %) and reduce CO_2 emissions in fossil fired boiler/steam turbine power plants
- **Solutions:**
  - Ni-Base Superalloys: too costly
  - FeCrAl alloys: bcc structure, weak >500 °C
  - Al_2O_3 coatings or surface treatments
  - Alumina-Forming Austenitic Steels
    - Combination of creep and oxidation resistance
    - Lower cost (Lower nickel content)

www.siemens.com
Yamamoto, Y., et al.: Science, 2007, vol. 316(5823), pp. 433–36.
Yamamoto, Y., et al., Metallurgical and Materials Transactions A, 2011. 42(4): p. 922-931.

Alumina-forming Austenitic (AFA) Stainless Steels

- Combination of good oxidation resistance & creep resistance
  - Oxidation resistance achieved by the formation of protective, external alumina scale. (~3 wt.% Al)
  - f.c.c. matrix with intermetallic strengthening (Ni_3Al etc.)

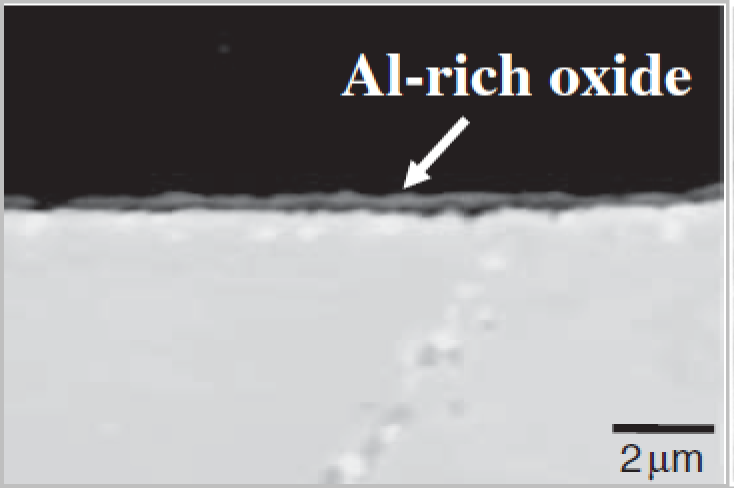

Fe-14Cr-20Ni-0.95Nb-2.5Al-2.5Mo wt. % base alloy (initial developed AFA)

BSE image after 72 hours of oxidation at 800°C in air

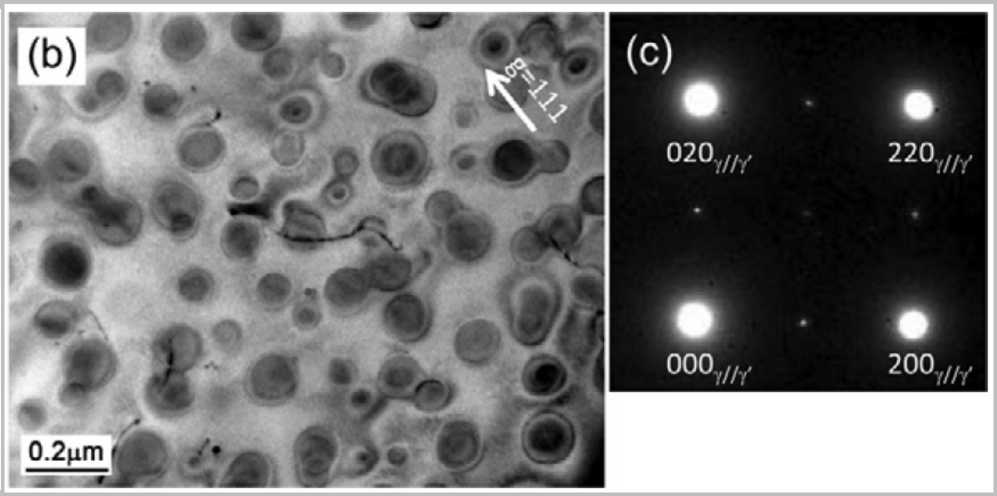

Fe-14Cr-32Ni-3Nb-3Al-2Ti wt.% base alloy (recent developed AFA)

TEM BF images of the alloys and SAD pattern

Yamamoto, Y., et al.: Science, 2007, vol. 316(5823), pp. 433–36.
Yamamoto, Y., et al., Scripta Materialia, 2013, 69(11–12), P.816–819.

Oxidation Resistance and Creep Performance of AFA Steels

- Alumina formation in AFA alloys
  - Others: Ti content, C and B addition
- The best alloy has >7 times longer creep life than A286

32ZCB: Fe–14Cr–32Ni–3Nb–3Al–2Ti-0.27Zr-0.14Si (wt.%)
41Z: Fe–14Cr–32Ni–3Nb–4Al–1Ti -0.27Zr-0.12Si (wt.%)

A286: Fe–14Cr–25Ni–2Ti-0.15Al (wt.%)

(Iron-base superalloy)

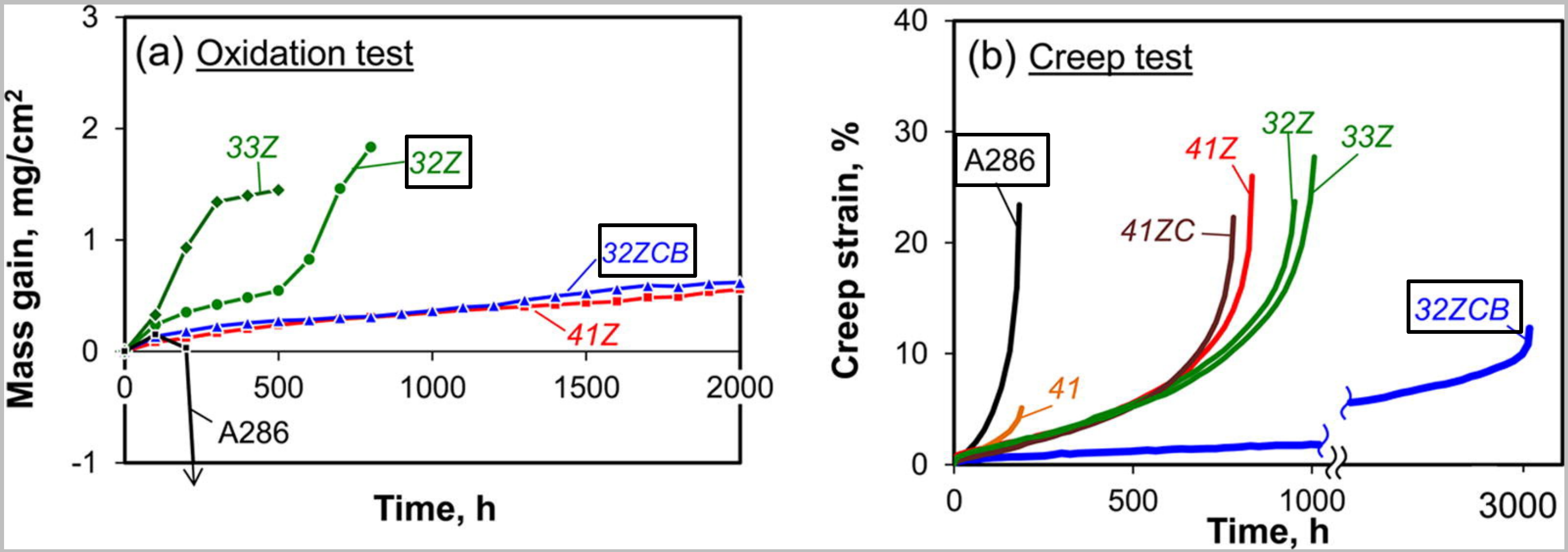

Cyclic oxidation test results at 800 °C in 10% water vapor

creep-rupture curves at 750 °C and 100 MPa.

Yamamoto, Y., et al., Scripta Materialia, 2013, 69(11–12), P.816–819.

Composition of Recent Developed AFA Steels

- Arc-melted 600 g ingot by using pure element feedstock.
  - Drop cast into 1” x 1” x 3” bar shape die.
  - Soaked at 1100 °C for 2 h in Ar + 4% H_2 gas
  - Hot-rolled the ingot along longitudinal axis for up to 80 % thickness reduction (~15-20 % thickness reduction per pass)
  - Anneal the plate at 1100 °C for 30 min in Ar + 4% H_2 gas, followed by air cooling.

Alloys	Fe	Cr	Ni	Al	Si	Nb	Ti	Zr	C	B
DAFA26	45.55	14	32	3	0.15	3	2	0.3		
DAFA29	45.44	14	32	3	0.15	3	2	0.3	0.1	0.01
A286	56.2	14.5	25	0.15	0.2	-	2.1	-	0.04	0.006

AFA alloys are supplied by Y. Yamamoto and M. P. Brady in Oak Ridge National Laboratory

SEM Analysis of DAFA26

- DAFA26: Fe-14Cr-32Ni-3Nb-3Al-2Ti-0.3Zr-0.15Si (wt.%) (as-hot-rolled)
  - Nb rich precipitates and grain size ~40 μm

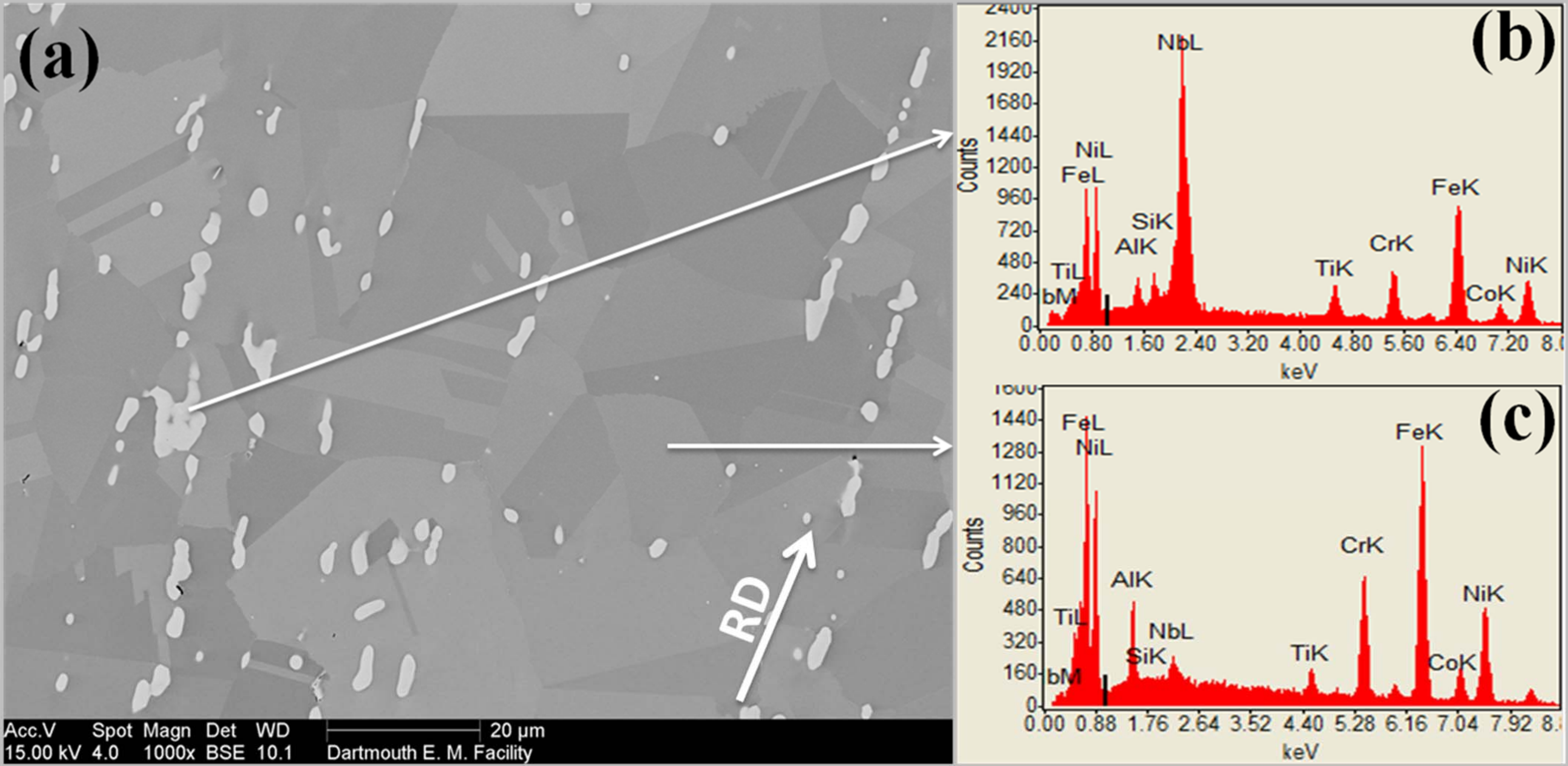

BF and CBED of Laves Phase in DAFA26

- DAFA26: Fe-14Cr-32Ni-3Nb-3Al-2Ti-0.3Zr-0.15Si (wt.%) (as-hot-rolled)
  - Fe$_2$Nb Laves phase precipitates + L1$_2$ precipitates in f.c.c. matrix

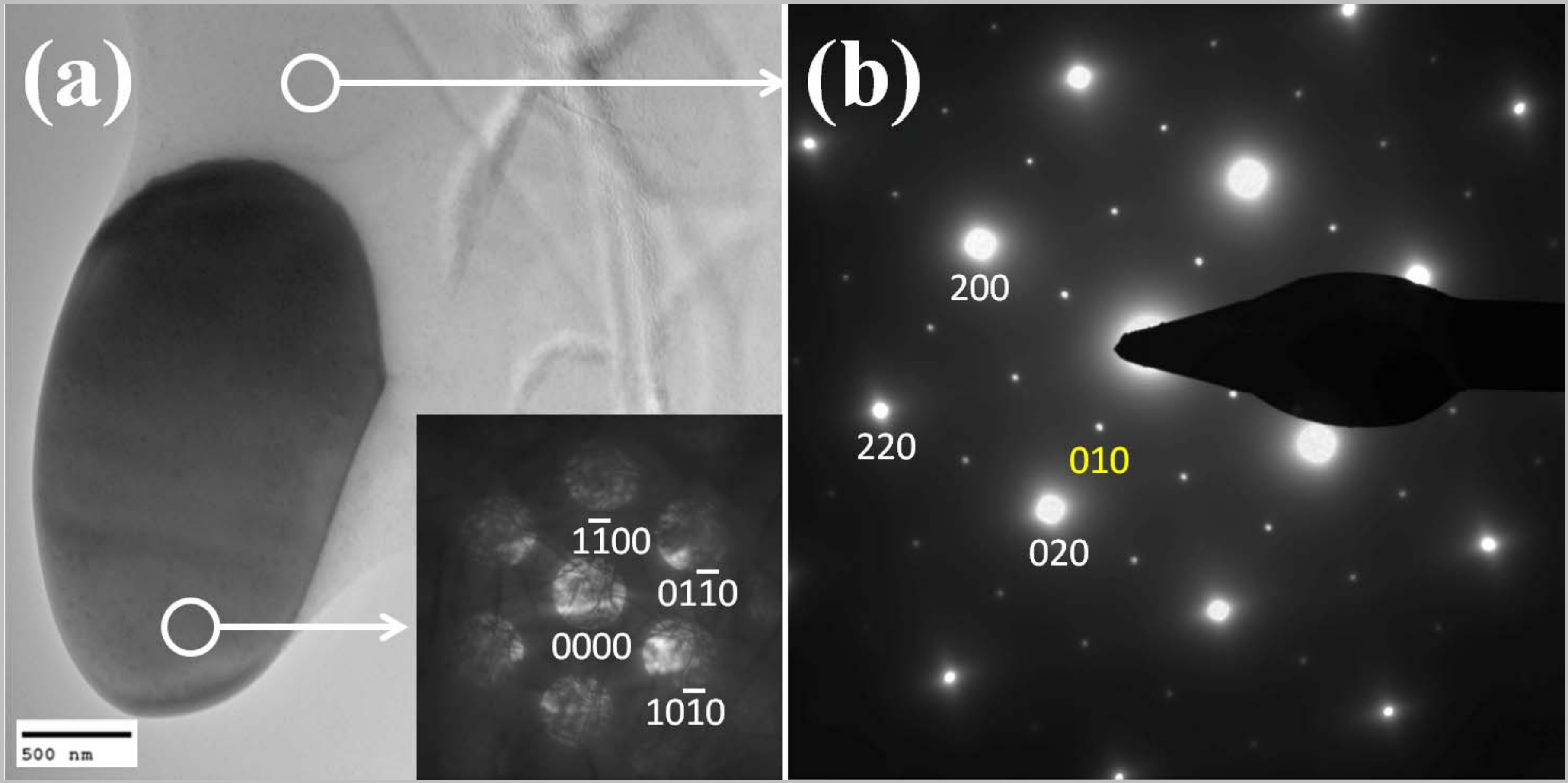

APT Analysis of DAFA26 (as-hot-rolled)

- DAFA26: Fe-14Cr-32Ni-3Nb-3Al-2Ti-0.3Zr-0.15Si (wt.%)

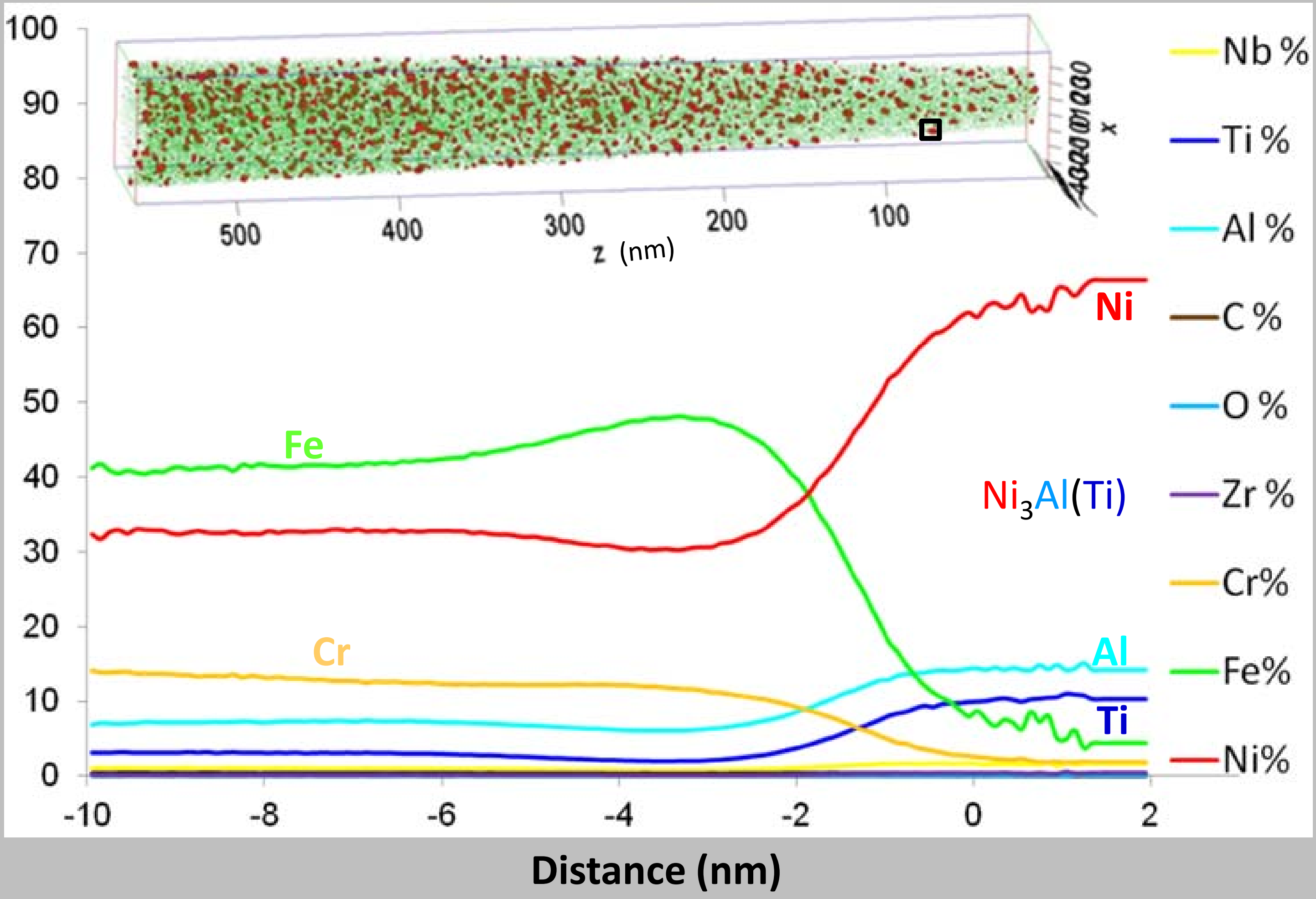

Collaboration with M. K. Miller in Oak Ridge National Laboratory

Thermo-mechanical Treatments Procedure

DAFA29: Fe-14Cr-32Ni-3Nb-3Al-2Ti-0.3Zr-0.15Si-0.1C-0.01B (wt.%) (recent developed)

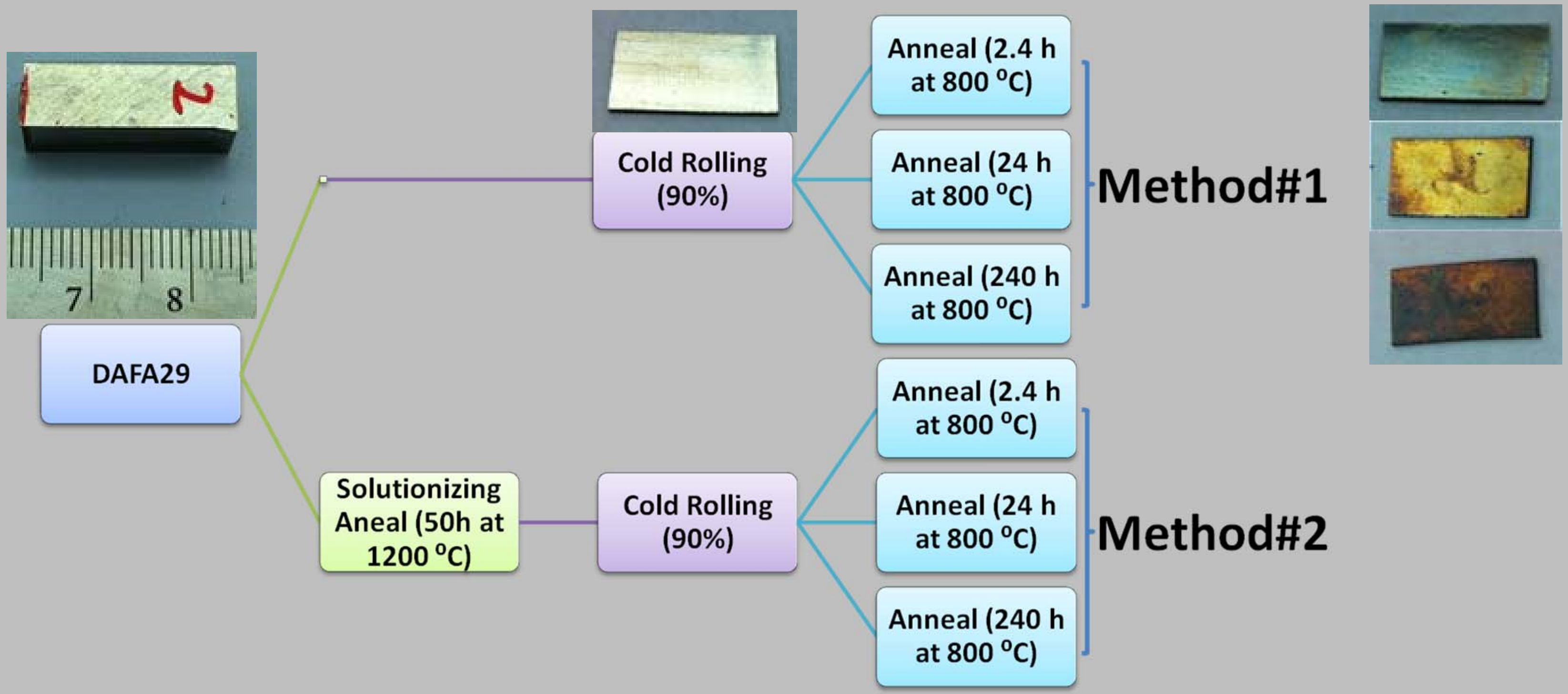

- Cold rolling 90 % thickness reduction (~4.5 % reduction per pass)
  - ❖ Enhance the creep properties
  - ❖ Introduce dislocations which will act as nucleation sites for precipitates and result longer creep life

BSE Images of DAFA29 after Thermo-mechanical Treatment Method#1

Method#1: DAFA29 + Cold Rolling (90%) + 800 ºC

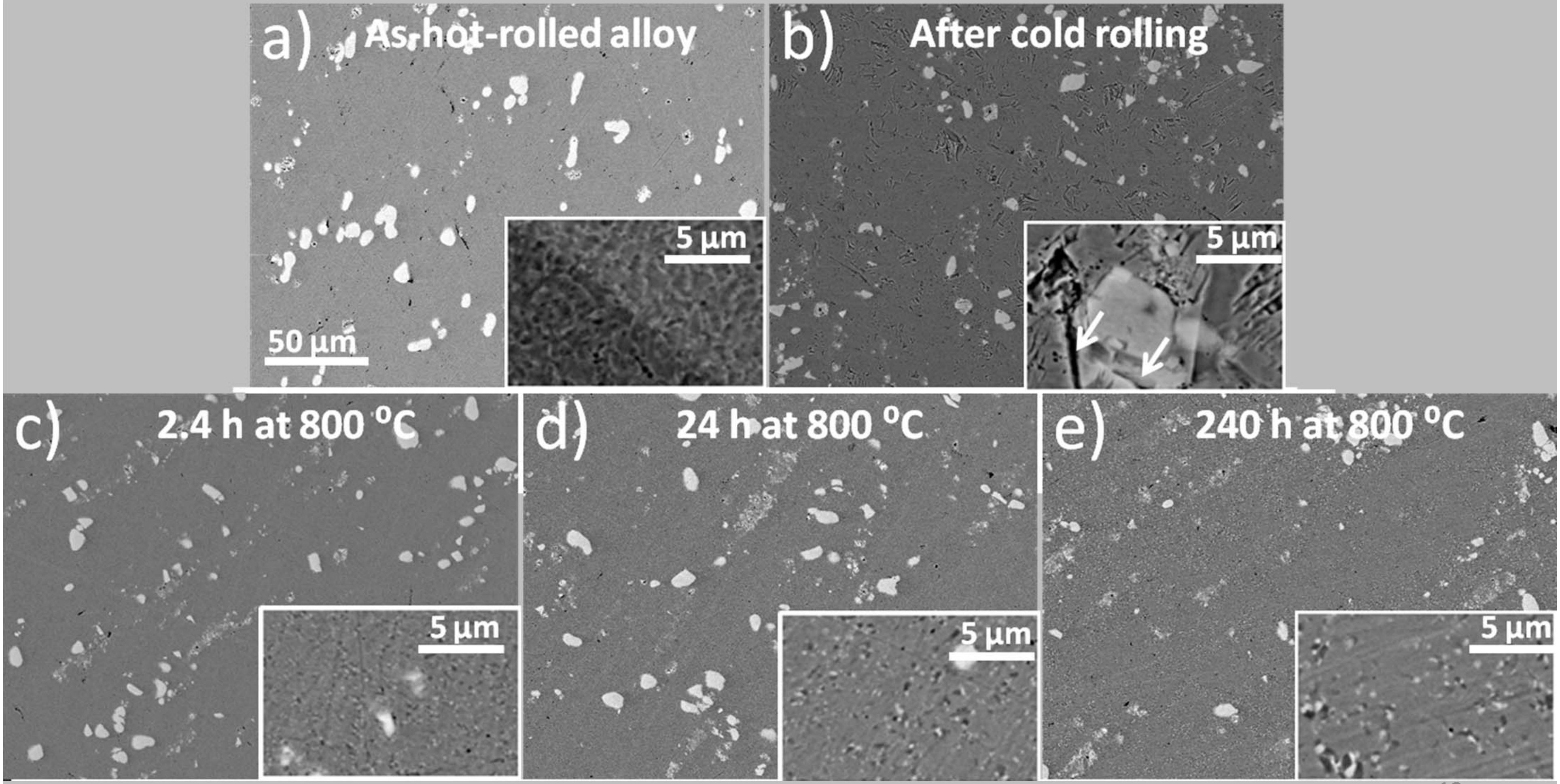

BSE Images of DAFA29 after Thermo-mechanical Treatment Method#2

Method#2: DAFA29 + 1200 ^{o}C (50h) + Cold Rolling (90%) + 800 ^{o}C

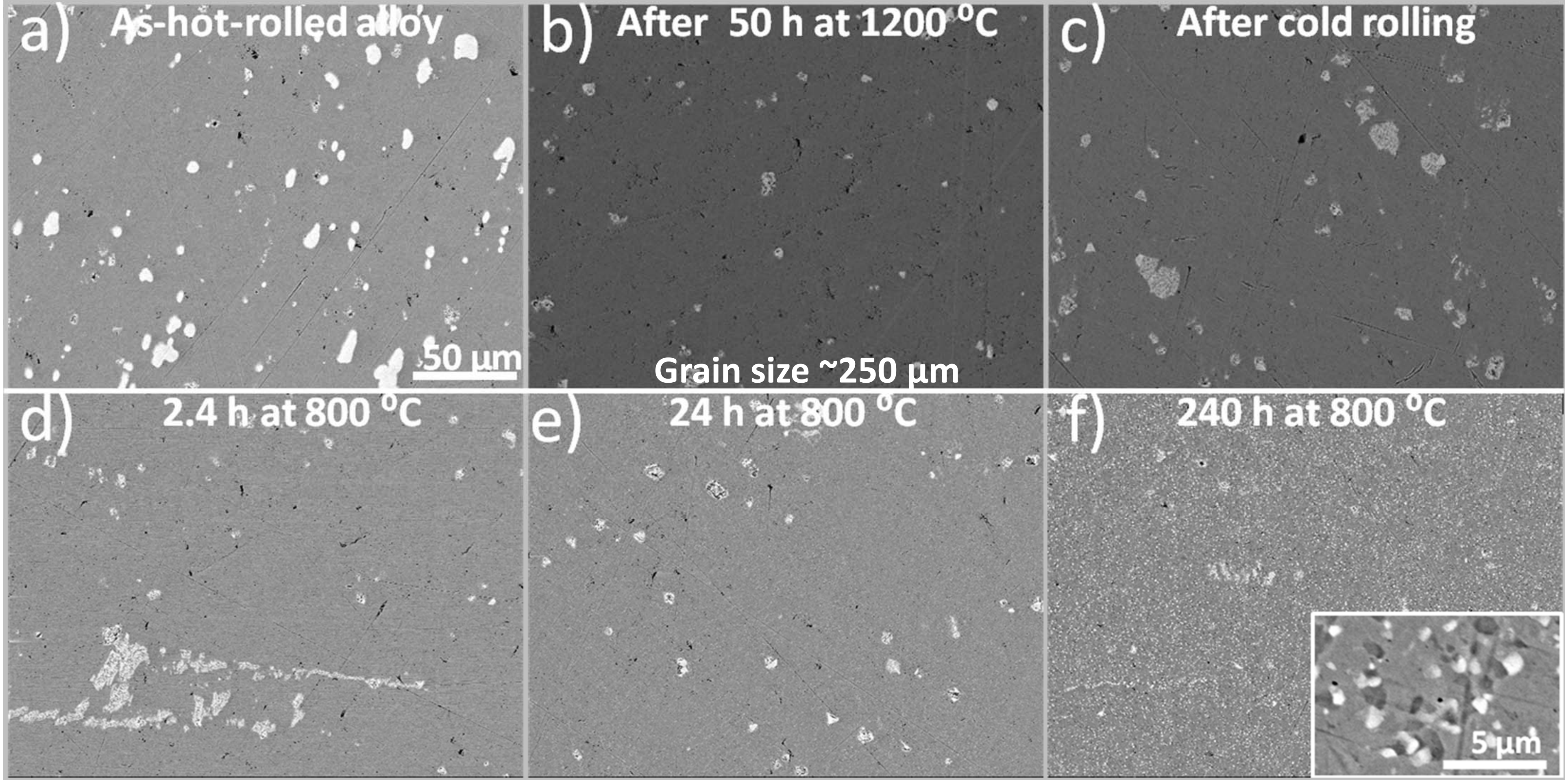

BF TEM Images and SAD of DAFA29 after Thermo-mechanical Treatment Method#1

Method#1: DAFA29 + Cold Rolling (90%) + 800 ^{o}C

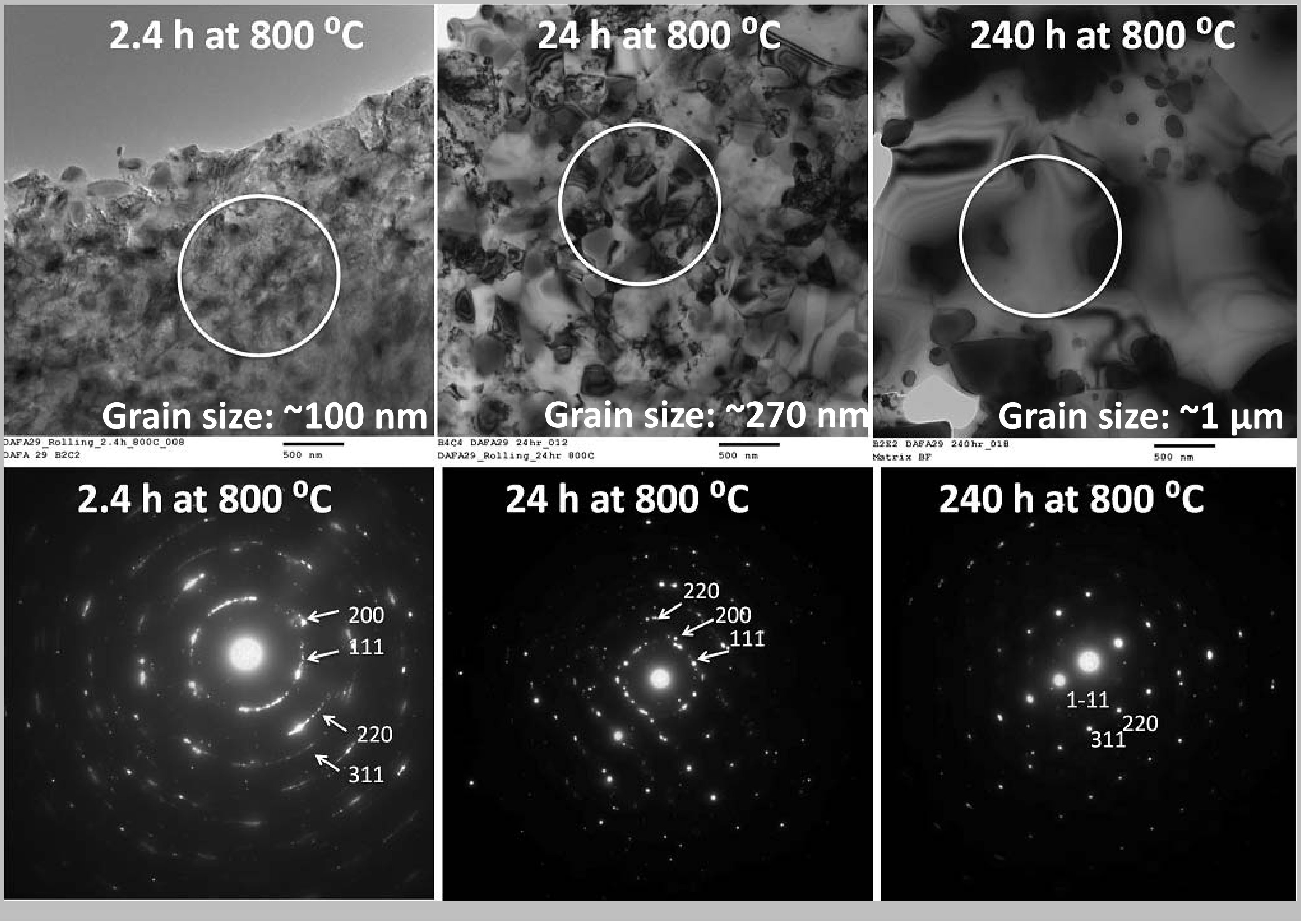

BF TEM Images and SAD of DAFA29 after Thermo-mechanical Treatment Method#2

Method#2: DAFA29 + 1200 °C (50h) + Cold Rolling (90%) + 800 °C

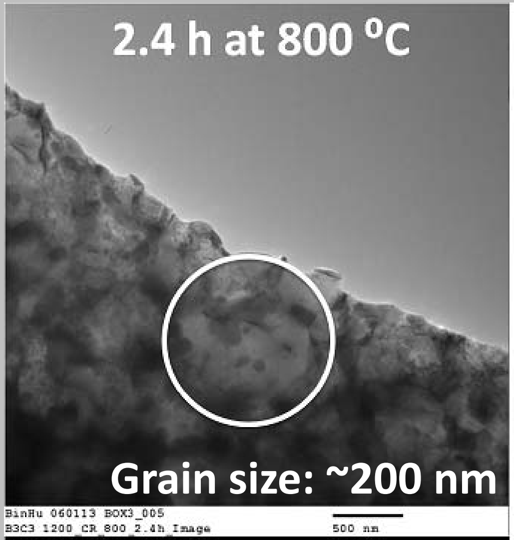
2.4 h at 800 °C

Grain size: ~200 nm

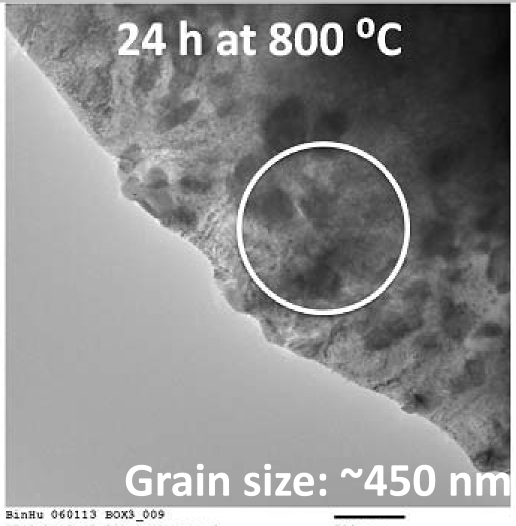
24 h at 800 °C

Grain size: ~450 nm

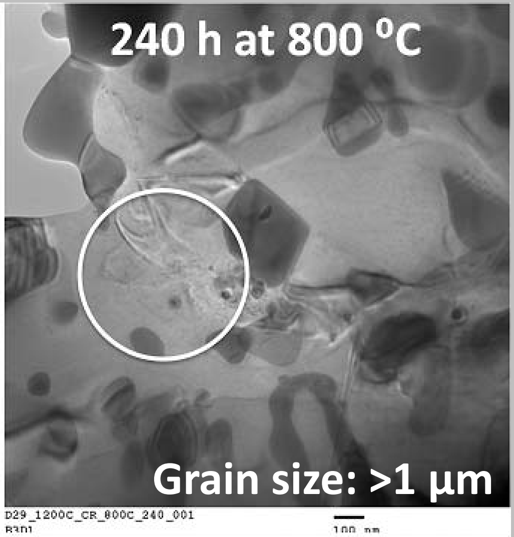
240 h at 800 °C

Grain size: >1 µm

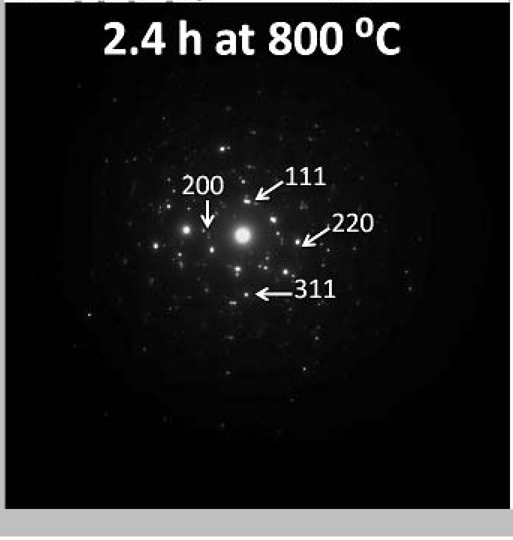
2.4 h at 800 °C

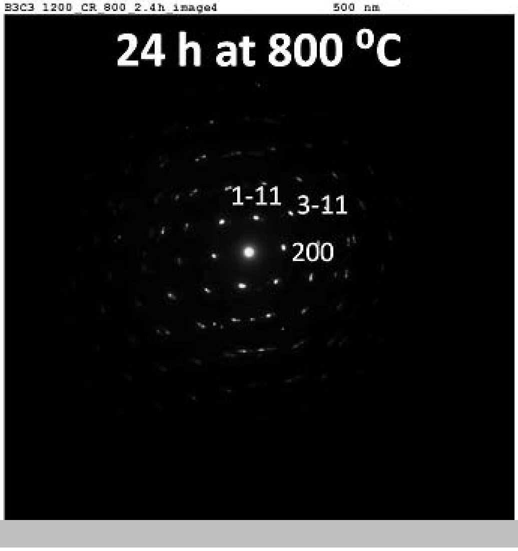
24 h at 800 °C

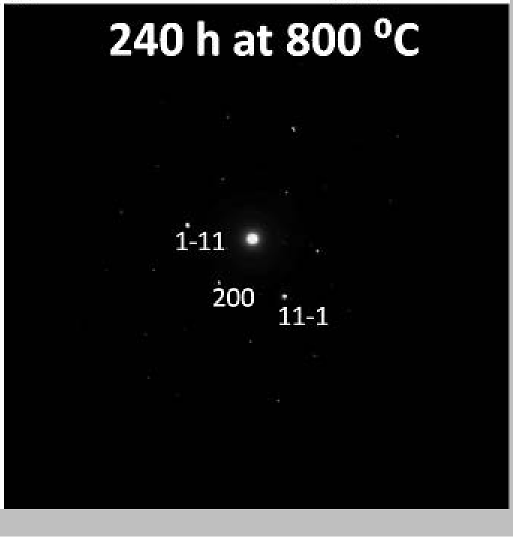
240 h at 800 °C

BF TEM image, EDS and CBED of a Laves Phase Precipitate in TMT DAFA29

- Fe_2Nb Laves phase precipitates
  - ❖ C14 structure, Fe:Nb = 2:1

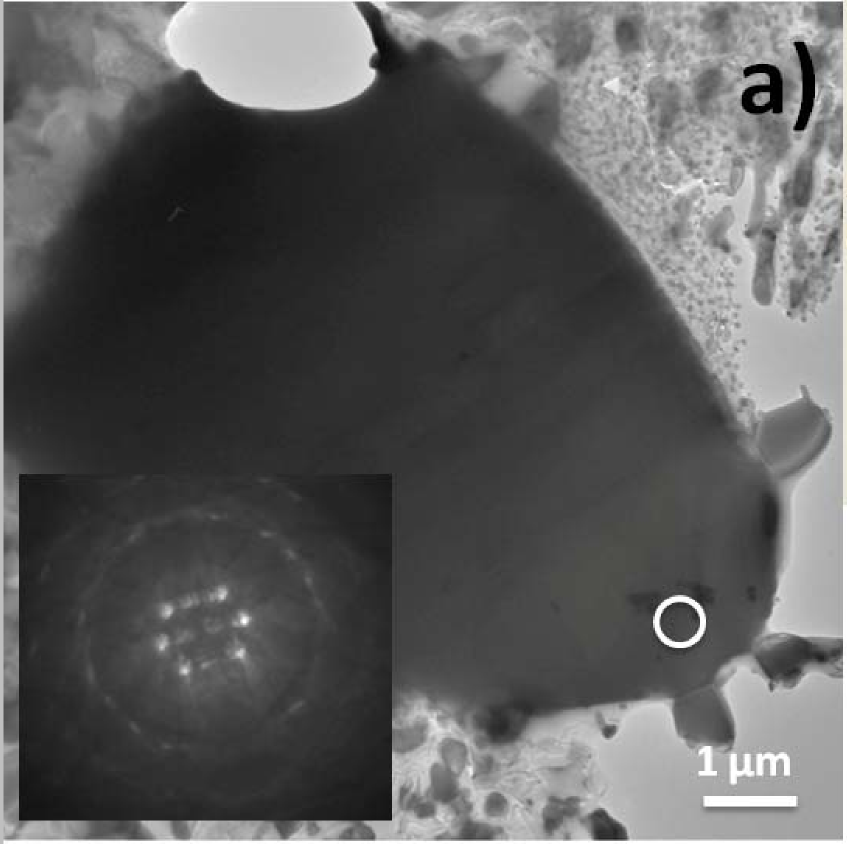

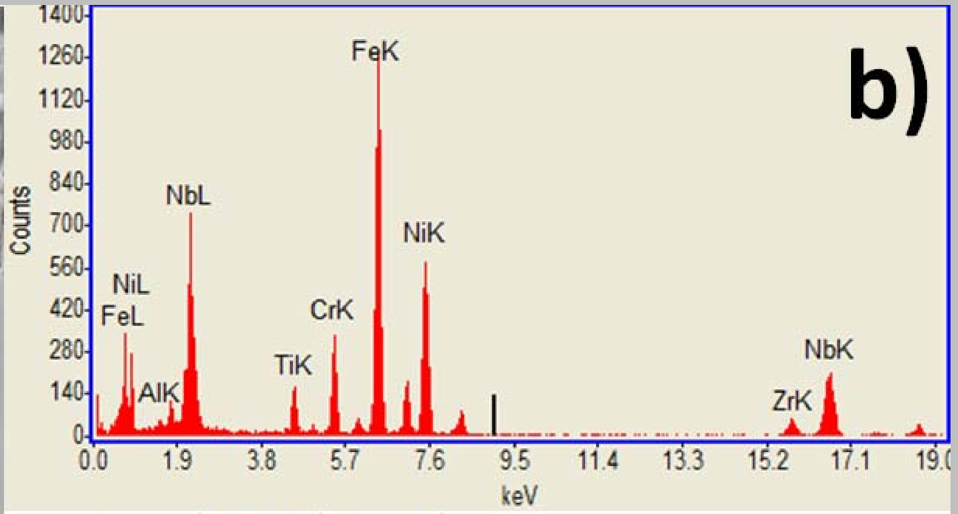

Elem	Weight %	Atomic %
AlK	0.6	1.5
TiK	3.2	4.3
CrK	7.7	9.5
FeK	36.2	41.5
NiK	17.9	19.5
ZrK	6.8	4.8
NbK	27.7	19.1
Total	100	100

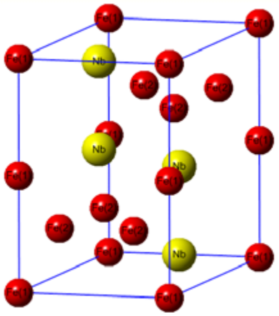

BF TEM Image, EDS and CBED of a B2 Precipitate in TMT DAFA29

- NiAl precipitates
  - B2 structure
  - Predicted B2 phase fractions: 5 % based on thermodynamic calculation

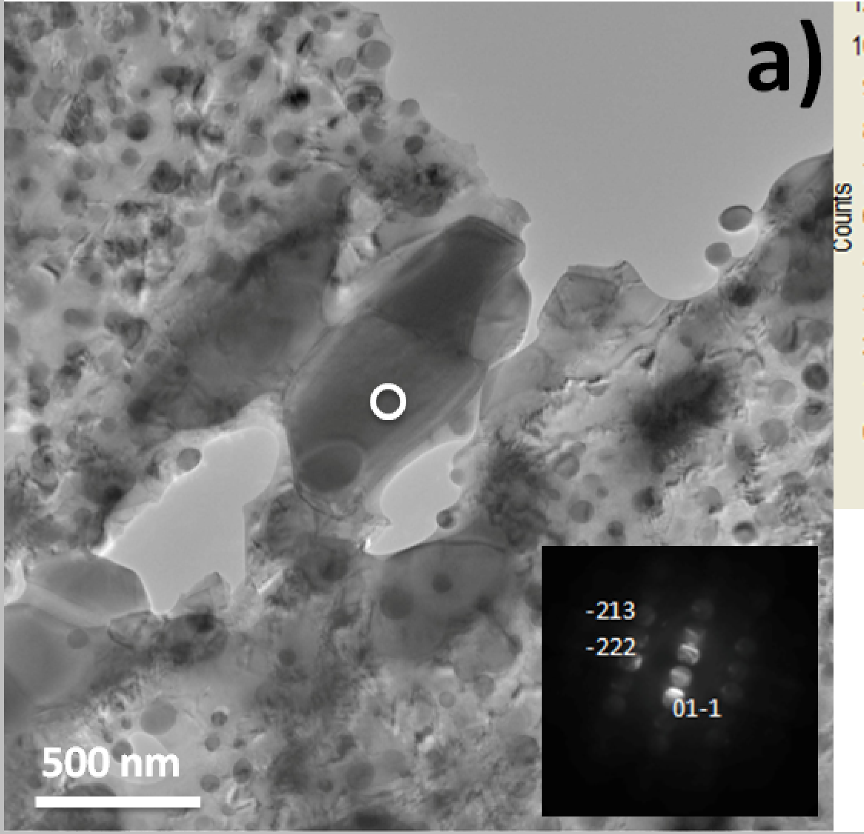

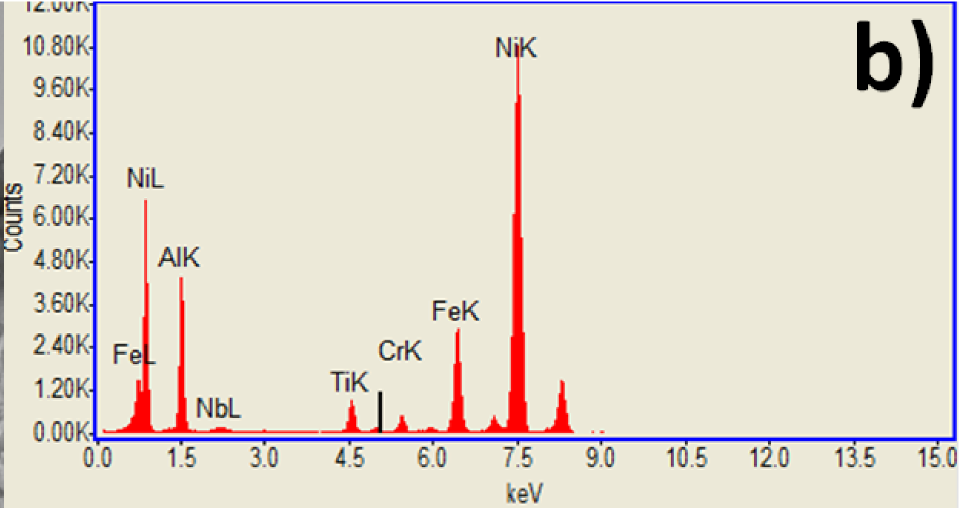

Elem	Weight %	Atomic %
AlK	14.1	26
NbL	1.2	0.6
TiK	3.5	3.7
CrK	1.9	1.8
FeK	13	11.6
NiK	66.3	56.2
Total	100	100

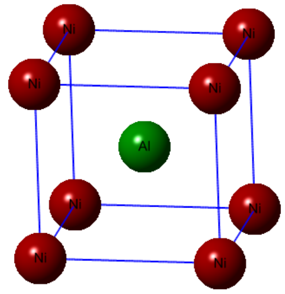

BF TEM Image, EDS and CBED of a $L1_2$ Precipitate in TMT DAFA29

- $Ni_3Al(Ti)$ type $L1_2$ precipitates
  - ❖ $L1_2$ structure, Ni:Al(Ti) = 3:1
  - ❖ Predicted $L1_2$ phase fractions: 21 % based on thermodynamic calculation

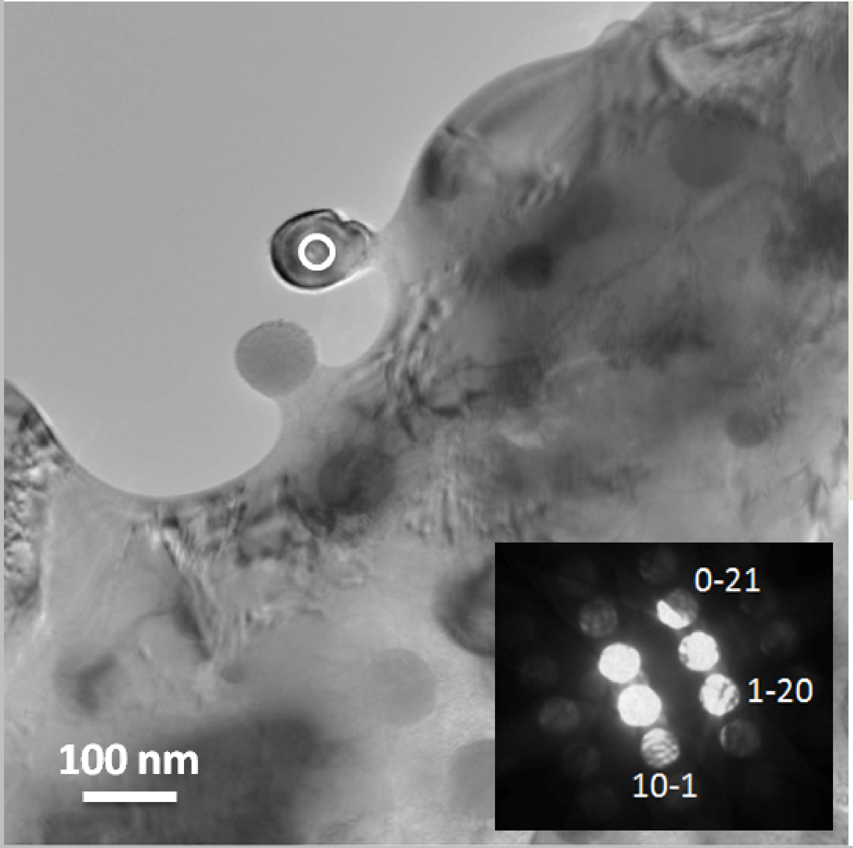

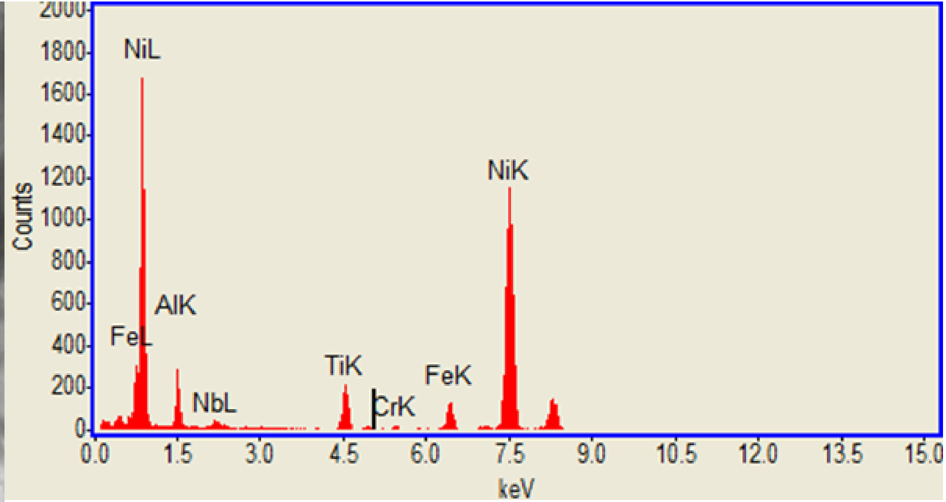

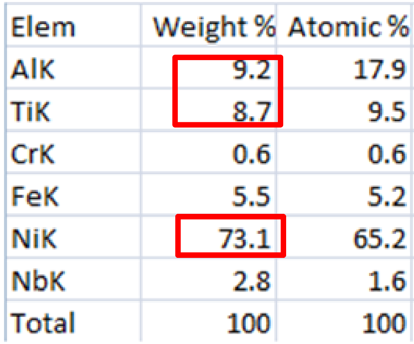

Elem	Weight %	Atomic %
AlK	9.2	17.9
TiK	8.7	9.5
CrK	0.6	0.6
FeK	5.5	5.2
NiK	73.1	65.2
NbK	2.8	1.6
Total	100	100

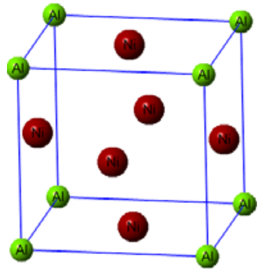

SE Image and BF TEM Image of $Ni_3Al(Ti)$ type $L1_2$ Precipitates

- Morphology of $Ni_3Al(Ti)$
  - Cold Rolling (90%) + 800 °C (240 h)

SE Image

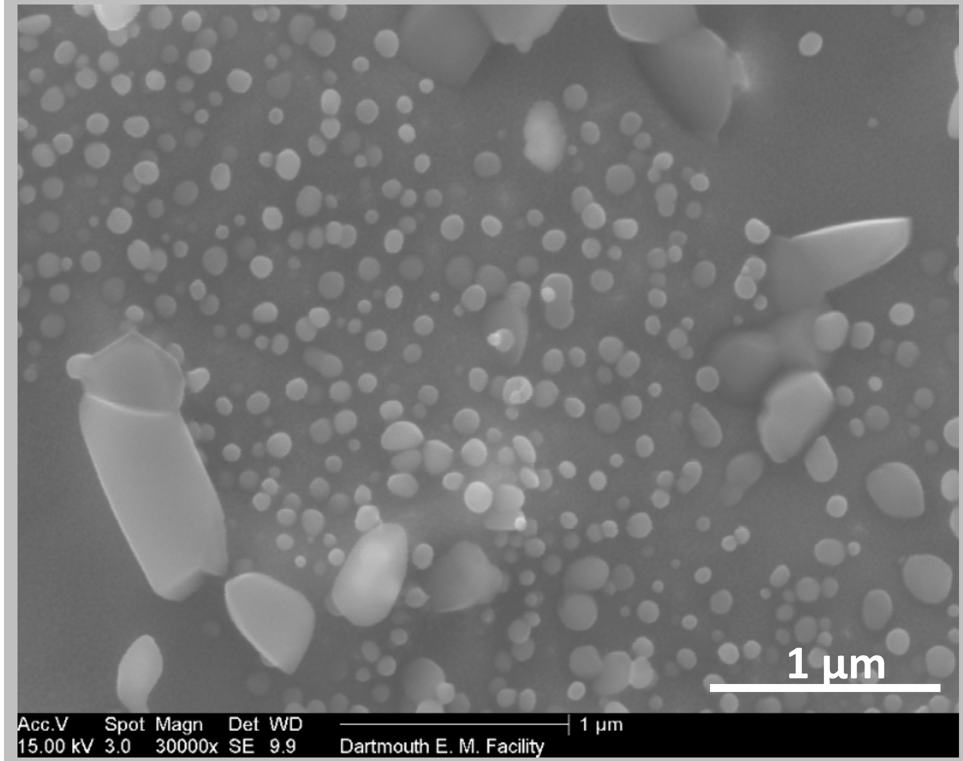

BF TEM Image

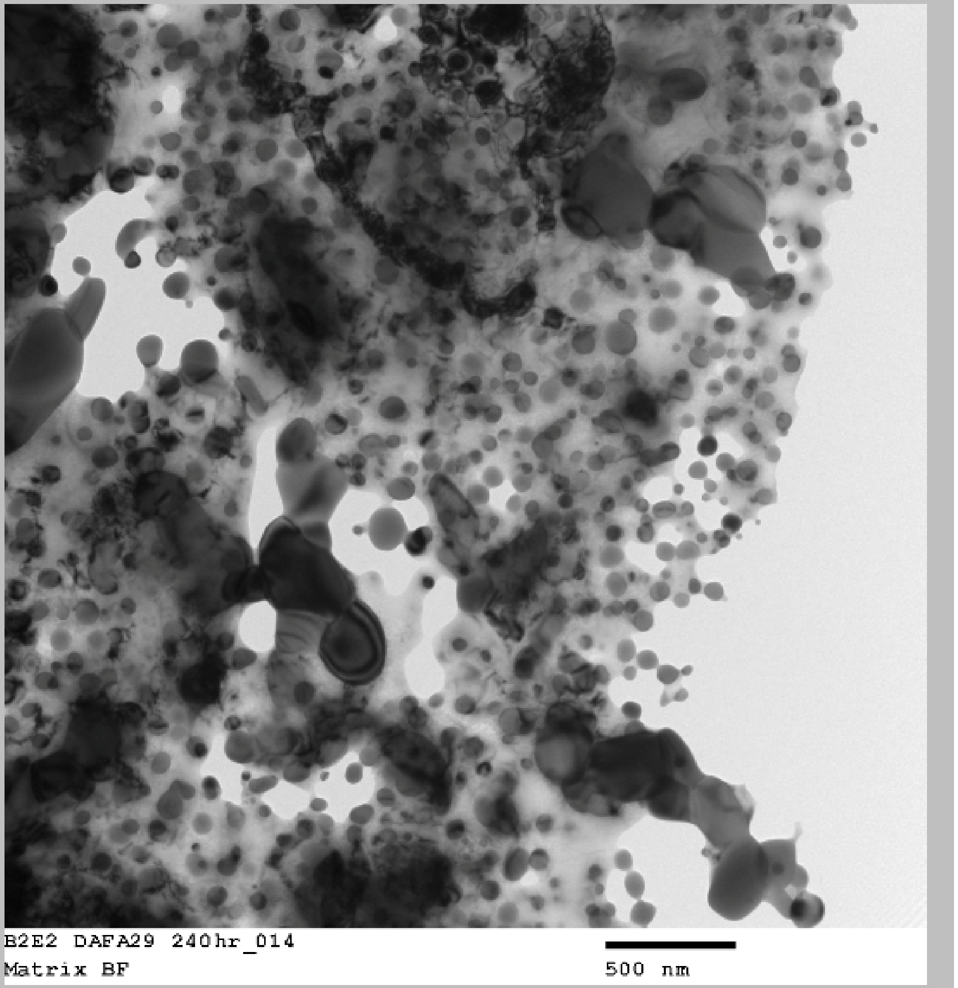

XRD and Synchrotron XRD Results

Method #1

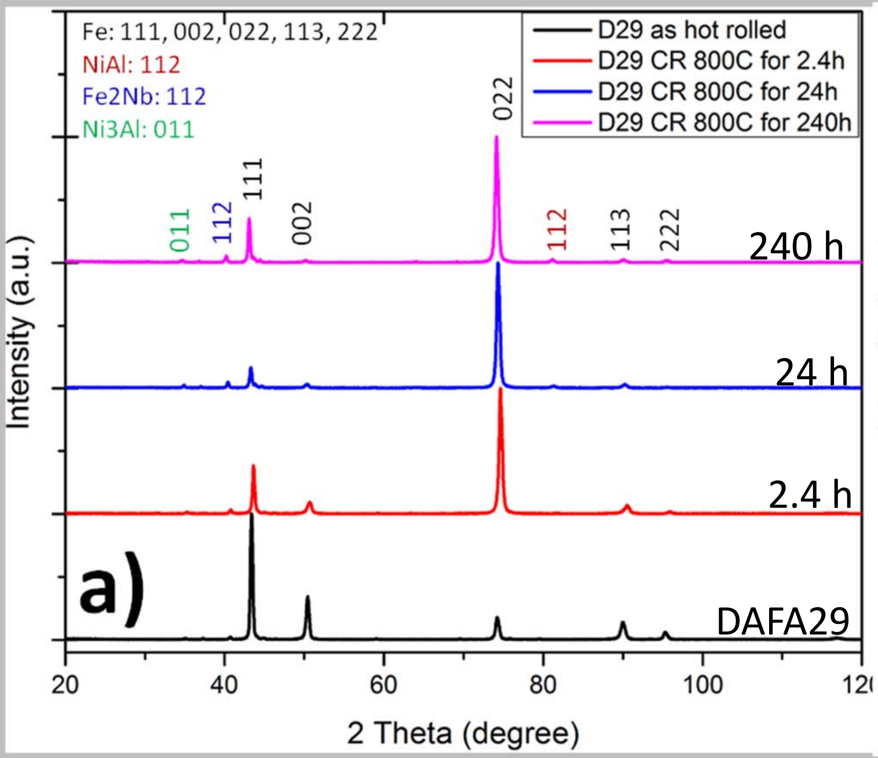

Method #2

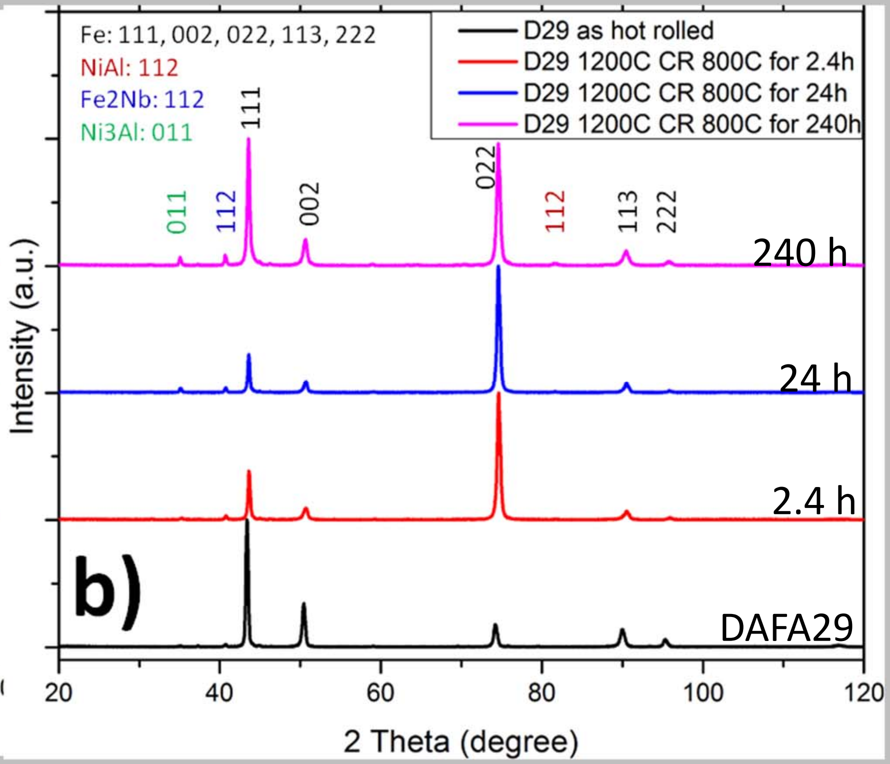

Lattice parameters

		Fe-f.c.c.	Fe_2Nb (a)	NiAl	Ni_3Al
	DAFA29	3.611	4.820	2.888	3.604
Method #1	**2.4 h**	3.599	4.812	2.883	3.590
	24 h	3.601	4.853	2.895	3.591
	240 h	3.597	4.881	2.900	3.587

Lattice parameters

		Fe-f.c.c.	Fe_2Nb (a)	NiAl	Ni_3Al
	DAFA29	3.611	4.820	2.888	3.604
Method #2	**2.4 h**	3.601	4.812	2.883	3.591
	24 h	3.601	4.817	2.888	3.594
	240 h	3.601	4.820	2.890	3.591

Lattice misfit of $L1_2$ phase with f.c.c. matrix is calculated to be only **~0.28%** for both treatments

Room Temperature Tensile Tests

Method #1

DAFA29 + Cold Rolling (90%) + 800 ^{o}C

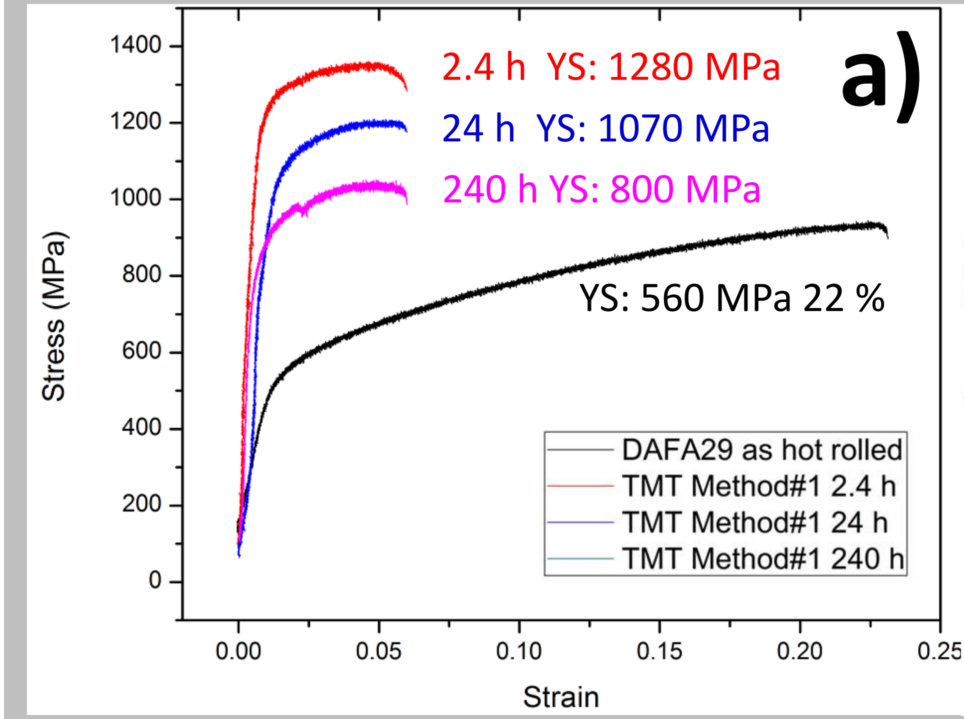

Method #2

DAFA29 + 1200 ^{o}C (50h) + Cold Rolling (90%) + 800 ^{o}C

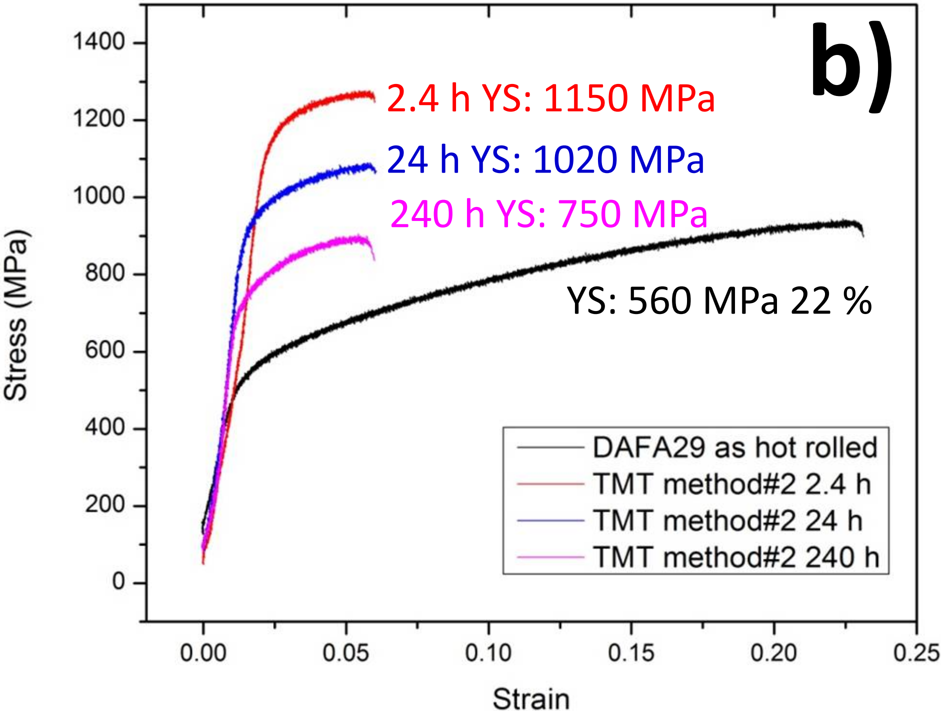

Hall-Petch: $\sigma_{0.2} = \sigma_0 + KD^{-0.5}$, where σ_0 = 600 MPa and K = 230 MPa•µm$^{-0.5}$

$$\sigma_0 = \boxed{\sigma_{ppt}} + \sigma_d + \sigma_{ss}$$

Tensile Tests of Control Samples

Method #1 Control
DAFA29 + 800 ^{o}C

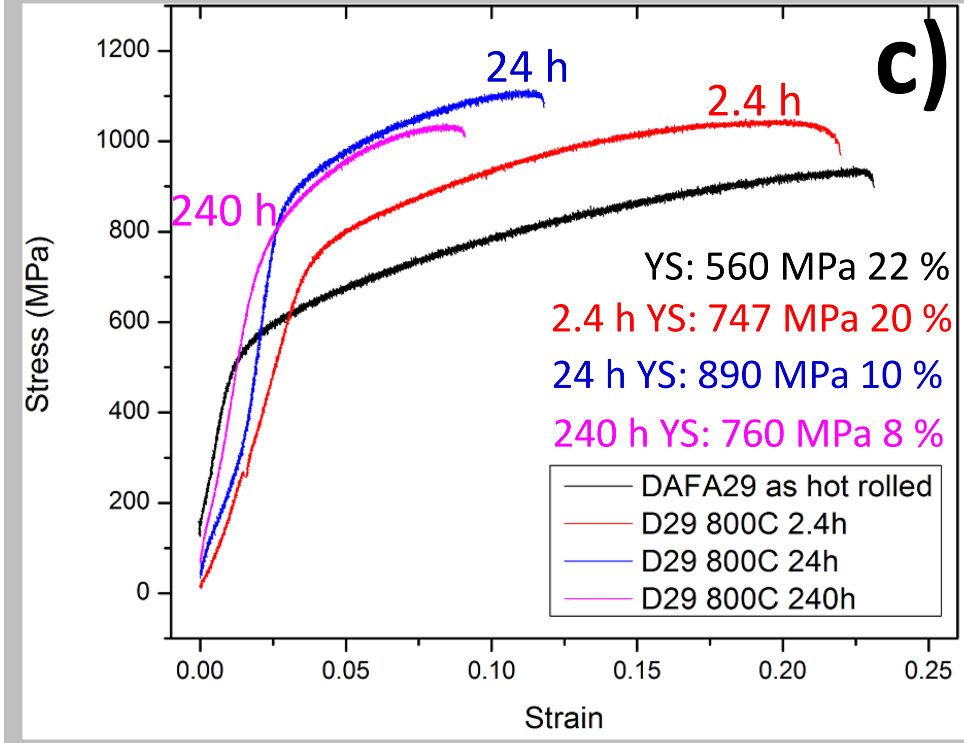

YS: 560 MPa 22 %
2.4 h YS: 747 MPa 20 %
24 h YS: 890 MPa 10 %
240 h YS: 760 MPa 8 %

Without Cold Rolling

Method #2 Control
DAFA29 + 1200 ^{o}C (50h) + 800 ^{o}C

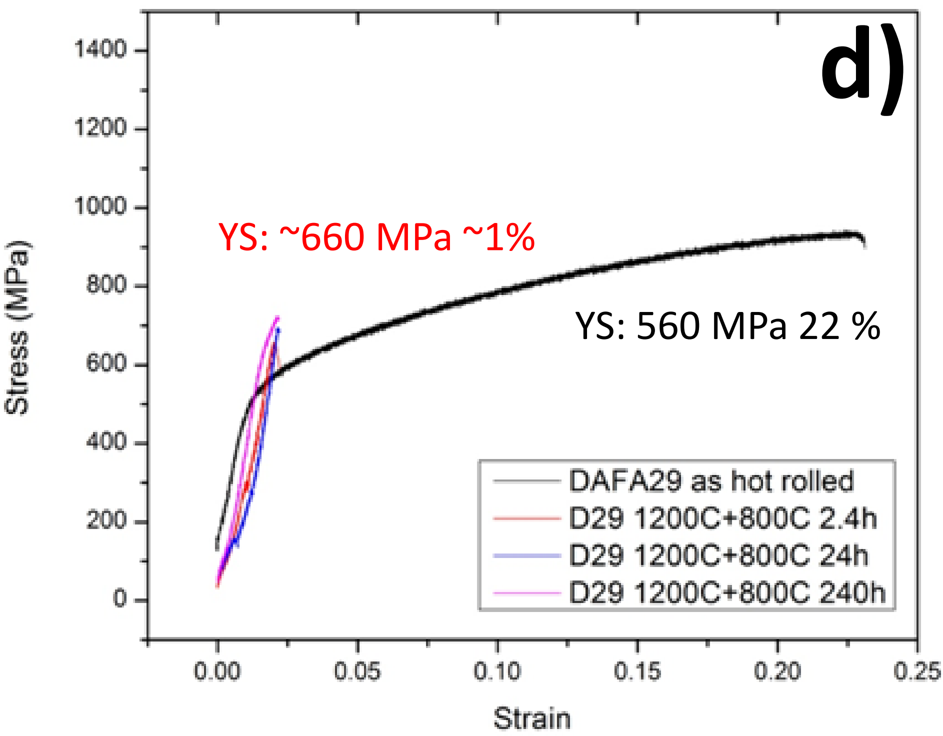

YS: ~660 MPa ~1%
YS: 560 MPa 22 %

Without Cold Rolling

BSE Images of Grain and Grain Boundaries in Control Samples

Method #1 Control: DAFA29 + 800 °C

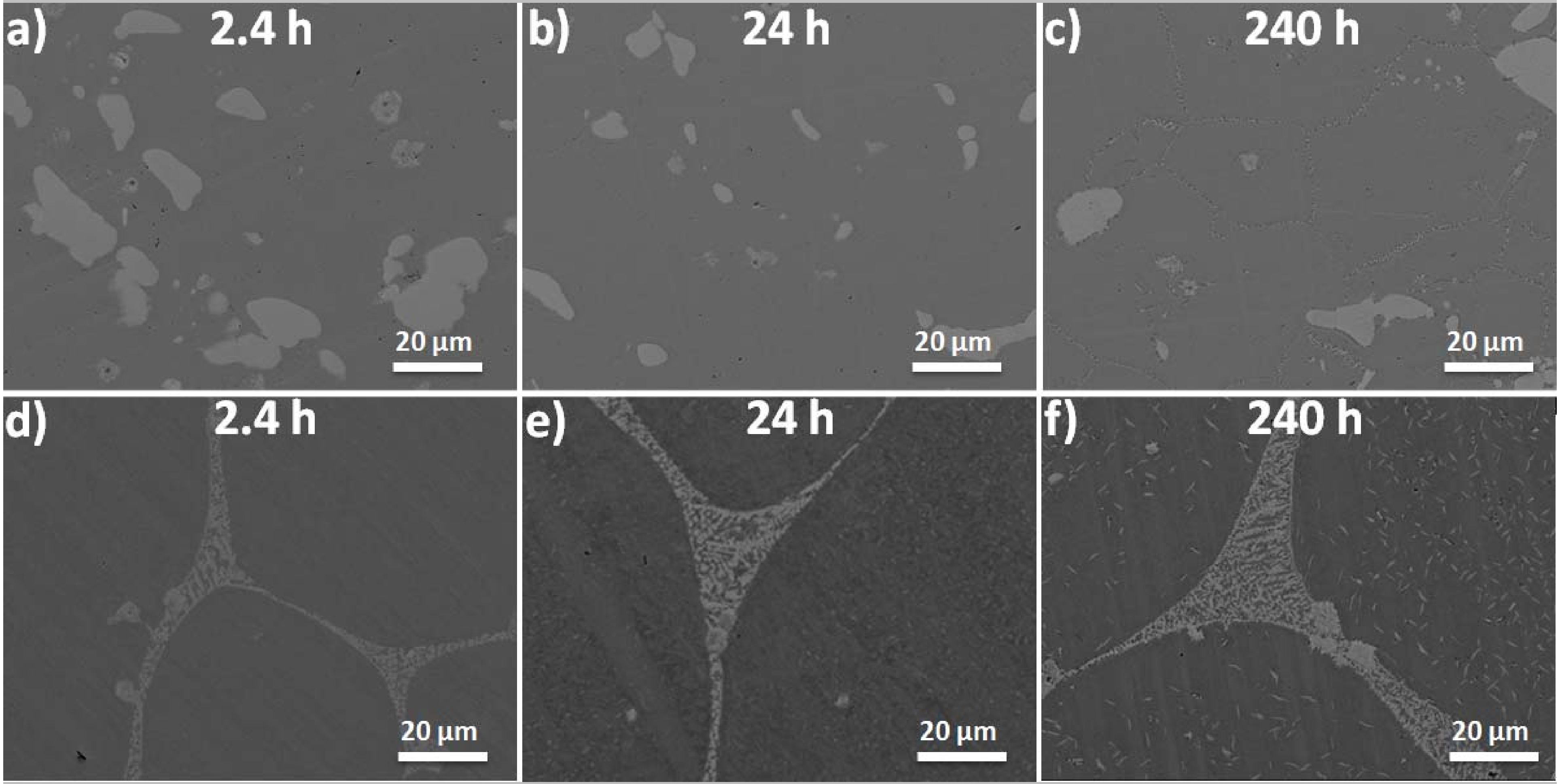

Method #2 Control: DAFA29 + 1200 °C (50h) + 800 °C

Ni_3Al Size Change after Method#1 Control 800 ºC Treatment

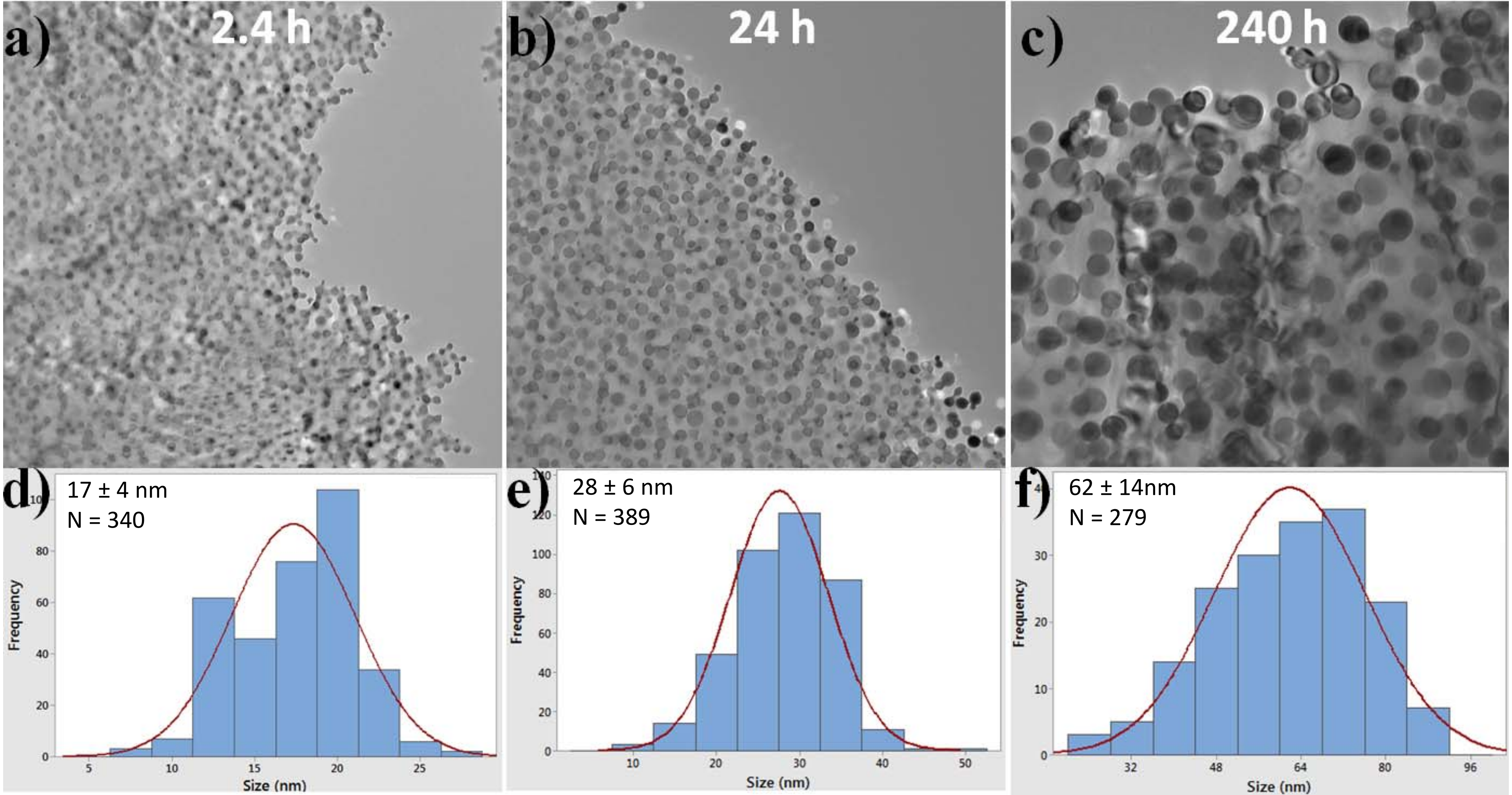

Ni$_3$Al Size Change after Method#2 Control 1200 °C (50h) + 800 °C Treatment

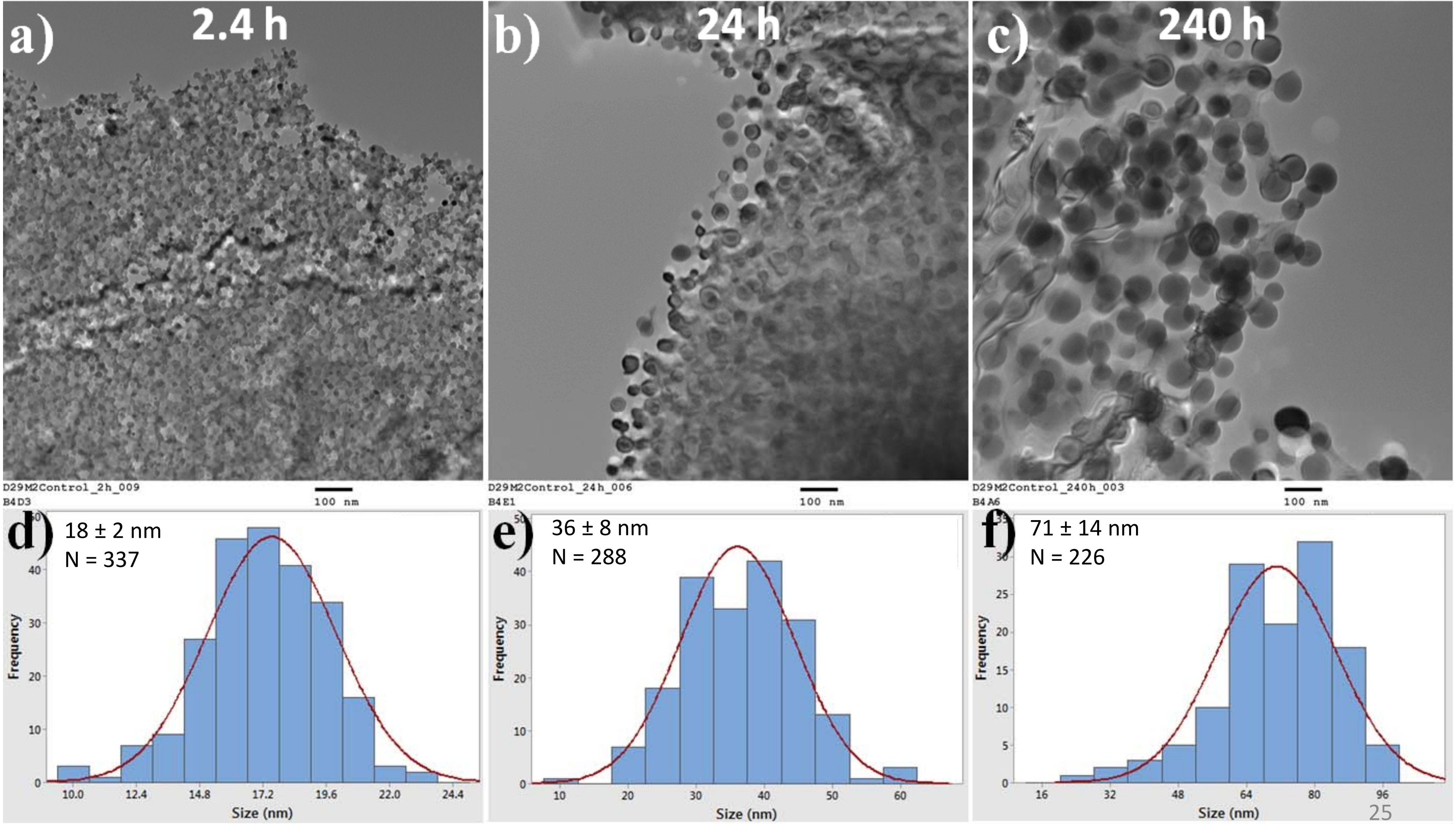

Summary

- A solutionizing anneal at 1200 ^{o}C followed by cold rolling and annealing at 800 ^{o}C can be used to generate a finer-scale and more uniform distribution of Laves phase precipitates.
- Cold rolling produces a high density of dislocations, which act as nucleation sites for Fe_2Nb Laves phase, B2 NiAl, and Ni_3Al precipitate formation
- Nanocrystalline steels processed through large strain cold rolling exhibit a dramatic increase in yield strength up to 1280 MPa. The yield strength decreases upon further annealing due to grain growth and precipitate coarsening.
- The yield strength of thermo-mechanically treated AFA steels exhibits a Hall-Petch relationship with a large value for σ_0 that likely arises from precipitate strengthening (σ_{ppt}).